New Practical Definitions for the Diagnosis of Autosomal Recessive Spastic Ataxia of Charlevoix–Saguenay

Julie Pilliod, PhD,[1] Sébastien Moutton, MD,[1,2] Julie Lavie, PhD,[1] Elise Maurat, BSc,[1] Christophe Hubert, BSc,[3] Nadège Bellance, PhD,[1] Mathieu Anheim, MD, PhD,[4,5,6] Sylvie Forlani, PhD,[7] Fanny Mochel, MD, PhD,[7,8] Karine N'Guyen, MD, PhD,[9] Christel Thauvin-Robinet, MD, PhD,[10] Christophe Verny, MD,[11] Dan Milea, MD,[12] Gaëtan Lesca, MD, PhD,[13] Michel Koenig, MD, PhD,[14] Diana Rodriguez, MD, PhD,[15,16,17] Nada Houcinat, BMedSc,[2] Julien Van-Gils, BMedSc,[2] Christelle M. Durand, PhD,[1] Agnès Guichet, MD,[18] Magalie Barth, MD,[18] Dominique Bonneau, MD,[18] Philippe Convers, MD,[19] Elisabeth Maillart, MD,[20] Lucie Guyant-Marechal, MD,[21] Didier Hannequin, MD, PhD,[21] Guillaume Fromager, MD,[22] Alexandra Afenjar, MD,[15,23] Sandra Chantot-Bastaraud, MD,[15,23] Stéphanie Valence, MD,[15,17] Perrine Charles, MD, PhD,[7] Patrick Berquin, MD, PhD,[24] Caroline Rooryck, MD, PhD,[1,2] Julie Bouron, BSc,[2] Alexis Brice, MD,[7,8] Didier Lacombe, MD,[1,2] Rodrigue Rossignol, PhD,[1] Giovanni Stevanin, PhD,[7,8,25] Giovanni Benard, PhD,[1] Lydie Burglen, MD, PhD,[15,16,23] Alexandra Durr, MD, PhD,[7,8] Cyril Goizet, MD, PhD,[1,2] and Isabelle Coupry, PhD[1]

View this article online at wileyonlinelibrary.com. DOI: 10.1002/ana.24509

Received Apr 4, 2015, and in revised form Aug 12, 2015. Accepted for publication Aug 14, 2015.

This article was published online on 14 November 2015. After online publication errors in Table 1 were corrected. This notice is included in the online and print versions to indicate that both have been corrected on 20 November 2015.

Address correspondence to Dr Coupry, Laboratoire Maladies Rares: Génétique et Métabolisme (MRGM), EA4576, 2ème étage Ecole de Sages-Femmes, Hôpital Pellegrin, Place Amélie Raba-Léon, 33076 Bordeaux cedex, France. E-mail: isabelle.coupry@u-bordeaux2.fr

From the [1]Rare Diseases Laboratory: Genetics and Metabolism, University of Bordeaux, Bordeaux, France; [2]Medical Genetics Service, Pellegrin University Hospital Center, Bordeaux, France; [3]Functional Genomics Center, University of Bordeaux, Bordeaux, France; [4]Neurology Service, Strasbourg University Hospitals, Strasbourg, France; [5]Molecular Cell Biology Genetics Institute, INSERM U964/CNRS UMR7104, University of Strasbourg, Illkirch-Graffenstaden, France; [6]Strasbourg Federation of Translational Medicine, University of Strasbourg, Illkirch-Graffenstaden, France; [7]Genetics Service, Pitié-Salpêtrière Hospital, Public Hospital Network of Paris, Paris, France; [8]Brain and Spinal Cord Institute, INSERM U1127, CNRS UMR7225, Sorbonne Universities–Pierre and Marie Curie University, Paris, France; [9]Department of Medical Genetics, Timone Hospital, Marseille, France; [10]Genetics Center, Dijon University Hospital Center, Dijon, France; [11]Nantes Angers le Mans University and Neurology Service, CNRS UMR6214, INSERM U1083, University Hospital Center, Angers, France; [12]Ophthalmology Service, Angers University Hospital Center, Angers, France and Singapore National Eye Centre, Singapore Eye Research Institute, Duke–National University of Singapore, Singapore; [13]Genetics Service, Lyon University Hospital Center, Lyon, France; [14]Molecular Genetics Laboratory, INSERM U827, Montpellier Regional University Hospital Center, Montpellier, France; [15]Rare Diseases Reference Center "Defects and Congenital Diseases of the Cerebellum," Armand Trousseau Hospital, Public Hospital Network of Paris, Paris, France; [16]Robert Debré Hospital, INSERM U1141, Paris, France; [17]Genetics Service, Armand Trousseau Hospital, Public Hospital Network of Paris, Paris, France; [18]Neuropediatrics Service, Armand Trousseau Hospital, Public Hospital Network of Paris, Sorbonne Universities–Pierre and Marie Curie University, Paris, France; [19]Nantes Angers le Mans University and Department of Biochemistry and Genetics, University Hospital Center, Angers, France; [20]Clinical Neurophysiology Service, Saint-Étienne University Hospital Center, Saint-Étienne, France; [21]Neurology Service, Pitié-Salpêtrière Hospital, Public Hospital Network of Paris, Paris, France; [22]Clinical Genetics Unit, Rouen University Hospital Center, Rouen, France; [23]Neurologist, Caen, France; [24]Amiens University Hospital Center, Pediatric Neurology Activity Center, Amiens, France; and [25]Laboratory of Neurogenetics, Practical School of Higher Studies, Paris, France

Additional Supporting Information may be found in the online version of this article.

Objective: Autosomal recessive spastic ataxia of Charlevoix–Saguenay (ARSACS) is caused by mutations in the *SACS* gene. *SACS* encodes sacsin, a protein whose function remains unknown, despite the description of numerous protein domains and the recent focus on its potential role in the regulation of mitochondrial physiology. This study aimed to identify new mutations in a large population of ataxic patients and to functionally analyze their cellular effects in the mitochondrial compartment.
Methods: A total of 321 index patients with spastic ataxia selected from the SPATAX network were analyzed by direct sequencing of the *SACS* gene, and 156 patients from the ATAXIC project presenting with congenital ataxia were investigated either by targeted or whole exome sequencing. For functional analyses, primary cultures of fibroblasts were obtained from 11 patients carrying either mono- or biallelic variants, including 1 case harboring a large deletion encompassing the entire *SACS* gene.
Results: We identified biallelic *SACS* variants in 33 patients from SPATAX, and in 5 nonprogressive ataxia patients from ATAXIC. Moreover, a drastic and recurrent alteration of the mitochondrial network was observed in 10 of the 11 patients tested.
Interpretation: Our results permit extension of the clinical and mutational spectrum of ARSACS patients. Moreover, we suggest that the observed mitochondrial network anomalies could be used as a trait biomarker for the diagnosis of ARSACS when *SACS* molecular results are difficult to interpret (ie, missense variants and heterozygous truncating variant). Based on our findings, we propose new diagnostic definitions for ARSACS using clinical, genetic, and cellular criteria.
ANN NEUROL 2015;78:871–886

First described 40 years ago in the regions of Charlevoix and Saguenay-Lac-St-Jean in Quebec, Canada, autosomal recessive spastic ataxia of Charlevoix–Saguenay (ARSACS) (Online Mendelian Inheritance in Man database [OMIM] #270550) is classically characterized by a triad of slowly progressive early onset cerebellar ataxia, lower limb pyramidal tract features (spasticity and Babinski signs), and axonal-demyelinating sensorimotor peripheral neuropathy.[1–5] The clinical spectrum of typical features also includes retinal changes, urinary symptoms, progressive cerebellar atrophy, and linear hypointensities in the pons on brain magnetic resonance imaging (MRI), which are considered hallmarks of the disease.[6–8] Studies have revealed that ARSACS is present worldwide with variable prevalence and phenotypic expression.[4,5,9]

ARSACS is caused by mutations in *SACS*, a large gene with a coding region >12kb, located on chromosome 13q12.12.[10,11] More than 100 mutations have been described to date, essentially leading to a premature stop codon.[9,12] The encoded protein sacsin is composed of several domains: ubiquitin-like, Hsp90-like, XPCB, DnaJ, HEPN, and the sacsin repeating region,[11–14] but its precise function remains largely unknown. Sacsin was first shown to be cytoplasmic, with 30% localized at or near the cytoplasmic face of the mitochondria in SHSY-5Y cells.[13] A colocalization with mitochondrial markers was confirmed in cultured hippocampal neurons, COS-7, and HeLa cells.[15] The presence of baloon-like or bulbed mitochondria indicative of a hyperfused mitochondrial phenotype was also observed in immortalized fibroblasts of 2 patients homozygous for the truncating mutation c.8844delT, the major founder mutation in Quebec. Using 3-dimensional confocal reconstructions coupled to fluorescence recovery after photobleaching in SHSY-5Y, sacsin knockdown led to a more interconnected mitochondrial network. Moreover, a moderate decrease in tetramethylrhodamine methyl ester (TMRM), fluorescence intensity, and a slower MitoTracker fluorescence recovery compared to control suggested impaired mitochondrial energetic functions. Finally, knockdown of sacsin in cultured hippocampal neurons revealed aberrant clustering and accumulation of mitochondria in the soma and proximal dendrites as well as reduced dendritic density. Very recently, spinal cord motor neurons cultured from *Sacs*$^{-/-}$ knockout mice exhibited abnormal accumulation of non-phosphorylated neurofilament bundles with significant reduction in mitochondrial motility and elongated mitochondria.[16]

We report here screening for *SACS* mutation in a large series of 321 patients with spastic ataxia by direct sequencing and 156 patients with congenital ataxia by targeted and whole genome sequencing. In addition to refining the description of the clinical and mutational spectrum of ARSACS patients, we also analyzed the functional consequences of various mutations on the mitochondrial compartment. Our results prompted us to propose new practical diagnostic definitions aimed at validating variants of uncertain clinical significance (VUS) as pathogenic mutations to establish a definite diagnosis of ARSACS.

Subjects and Methods

Subjects

A cohort of 321 patients with spastic ataxia was selected from the collection of the European and Mediterranean network for spinocerebellar degenerations (SPATAX, http://spatax.wordpress.com). Clinical criteria for inclusion of the patients were the presence of cerebellar ataxia and lower leg pyramidal tract involvement with an age at onset younger than 45 years and the absence of ataxia in the parental generation. In all cases, Friedreich ataxia was previously excluded.

In parallel, 156 patients suffering from congenital ataxia were investigated through the ATAXIC research project.

Clinical criteria for inclusion of the patients were early onset ataxia before age 2 years with stable evolution or progressive improvement at the time of inclusion.

One additional patient, 12436B-JAM-001, a 12-year-old girl suffering from congenital ataxia diagnosed at age 1.5 years, was included. Examination revealed severe ataxia with very slow ocular saccades. She had no intellectual deficiency. Brain MRI was normal. The course of neurological anomalies was stable over the years. Walking without support was possible, but running was impossible. A genomic 13q12.12 deletion of approximately 1.5Mb encompassing the whole *SACS* gene was identified on routine pan-genomic array comparative genomic hybridization (CGH; Human660-Quad v1.0 DNA Analysis BeadChip; Illumina, San Diego, CA). The diagnosis of ARSACS was then suspected.

All patients gave written informed consent to participate in genetic studies, according to the Declaration of Helsinki. The investigations fulfilled our institutions' ethical rules for human studies (RBM 01-29, RBM 03-48 for SPATAX and Patient 12436B-JAM-001 and Ile de France IX ethics committee approval No. IDRCB 2010-A00715-34 for ATAXIC).

Cell Cultures

Fibroblasts were obtained from arm skin biopsies in 11 patients and in 8 healthy controls including 5 females (18, 25, 26, 27, and 46 years old) and 3 males (21, 43, and 54 years old). Primary culture cells (patient and control fibroblasts) were cultured at 37°C in 5% CO_2 in glucose medium consisting of Dulbecco modified Eagle medium (DMEM) supplemented with 10% fetal bovine serum and 100U/ml penicillin/streptomycin. All the experiments were performed on cultures between the 3- and 5-passage stages. For mitochondrial analysis, subconfluent cells were trypsinized and counted on a Malassez cell counter and 20,000 cells were grown in glucose medium on a 4-well Lab-Tek (Thermo Scientific, Waltham, MA) plate for 24 hours prior to the experiments.

Mutation Screening

SACS DIRECT SEQUENCING. The coding sequence and exon–intron boundaries of the 9 coding exons of *SACS* (GenBank accession number NM_014363.5) were amplified by polymerase chain reaction (PCR). The amplicons were sequenced in both directions using the Big Dye Terminator Cycle Sequencing Kit v1 (Applied Biosystems [ABI], Foster City, CA) by using an ABI Prism 3130XL automated sequencer. The electrophoretic profiles were analyzed with Seqscape v2.7 (ABI). Primers sequences and conditions for PCR and sequencing are available from the authors upon request. After identification of a variant, reamplification and resequencing were systematically performed in a new DNA aliquot, and segregation with the disease was verified by direct sequencing of the mutated amplicons in additional family members when available. Variant nomenclature was based on the *SACS* transcript reference NM_014363.5. The mutation numbering system was based on cDNA or protein sequence as suggested by the internationally agreed mutation nomenclature (www.hgvs.org/).

NEXT GENERATION SEQUENCING. To search for disease-causing mutations in patients presenting with congenital ataxia, either targeted (144 patients) or whole exome (12 patients born from consanguineous parents) sequencing was used.

Targeted sequencing intended to search for mutations in 35 genes (*GRID2, WDR81, ABCB7, ATCAY, CAMTA1, CA8, ZNF592, CACNA1A, ADCK3, SACS, SIL1, KIAA0226, ATP2B3, GRM1, ITPR1, SLC2A1, SPTBN2, KCNC3, TSEN54, POLG, KCNJ10, POLR3A, POLR3B, TSEN2, TSEN34, EXOSC3,* and 9 candidate genes) involved in various forms of ataxia was performed by using the Access Array device from Fluidigm (South San Francisco, CA; PCR multiplex method using a microfluidic support) optimized by IntegraGen to increase the level of multiplexing. Thus, 48 pools of 48 PCRs for 48 samples were designed, allowing us to obtain 110,592 amplifications by Access Array and 2,304 amplicons per sample. PCR products from each sample corresponding to the different libraries were sequenced on a MiSeq Sequencer (Illumina).

Whole exome sequencing was performed using Agilent in-solution enrichment methodology to capture 50Mb exons (SureSelect Human All Exon v5 kit; Agilent Technologies, Santa Clara, CA), followed by 75 paired-end bases massively parallel sequencing on an HiSEQ 2000 (Illumina). The Illumina pipeline used for bioinformatics analysis included CASAVA1.8.2 allowing alignment of reads to a reference genome (hg19), calls of single nucleotide polymorphisms (SNPs) based on the allele calls and read depth, and detection of variants (SNPs and indels). The alignment algorithm used was ELANDv2 (which performs multiseed and gapped alignments). Only the positions included in the bait coordinates were conserved. Genetic variations annotation was performed from an IntegraGen in-house pipeline and consists of gene annotations (RefSeq), known polymorphisms (dbSNP [http://www.ncbi.nlm.nih.gov/SNP/] 132, 1000 Genomes, Exome Variant Server [EVS]), followed by a mutation characterization (eg, exonic, intronic, silent, nonsense). For each position, the exomic frequencies (homo- and heterozygotes) were determined from all the exomes already sequenced at IntegraGen, and the exome results provided by 1000 Genomes Project, EVS, and HapMap. Results were provided per sample in tabulated text files. We also performed a coverage/depth statistical analysis for the whole exome and exon per exon. Minimum average depth in the exome was around ×50. All the data could be visualized and filtered in ERIS (Exome Resequencing Intelligent Sorter), the Web interface developed by IntegraGen (http://eris.integragen.com/).

mRNA and cDNA Analyses

Extraction of total RNA from primary culture cells was performed using the RNeasy Mini Kit (Qiagen, Valencia, CA), using the separation method with QIAzol-chloroform following the manufacturer's instructions. Reverse transcription of 1 μg of total RNA was performed with the SuperScript double-strand

kit (Invitrogen, Carlsbad, CA) to obtain double-strand cDNA. cDNA was amplified by PCR in a thermal cycler (VWR International, Radnor, PA). Primer sequences and PCR conditions are available from the authors upon request. PCR products were separated on a 3% agarose gel.

Mitochondrial Morphology Analysis

The analysis of mitochondrial morphology was performed on living cells stained with MitoTracker Green (Invitrogen). Briefly, the cells were stained with MitoTracker Green 150 nM for 20 minutes at 37°C, and Z-stack imaging (1,000 μm) was performed on a Zeiss microscope (AxioVision) with a ×63 objective. The number of images was adapted to the width of each individual cell. Cells were grown in glucose medium on a 4-well Lab-Tek plate. One hundred cells per experimental condition (ARSACS patients vs control) were selected randomly, and the global mass of the mitochondrial network was evaluated. The fluorescence intensity of the mitochondrial network was measured with morphometric software (ImageJ; National Institutes of Health, Bethesda, MD). This allowed the region of interest to be manually selected and the area occupied by the selected pixels to be calculated.

Measuring Mitochondrial Membrane Potential

Mitochondrial membrane potential ($\Delta\Psi m$) was measured by quantification of TMRM (Invitrogen) fluorescence as described by Chazotte.[17] TMRM is a potential-sensitive dye used to measure $\Delta\Psi m$, which is generated by oxidative phosphorylation and is thus an indicator of mitochondrial function.[18,19] The probe, used here at a concentration of 5nM, was added to the cell medium and incubated for 20 minutes at 37°C. Cells were washed in phosphate-buffered saline, and fluorescence was quantified with MorphoPro software (Safran Morpho, Issy-les-Moulineaux, France).

Measuring Mitochondrial Respiration

The rate of mitochondrial respiration was measured in skin fibroblasts by polarography (OXY1; Hansatech Instruments, Norfolk, UK). The routine (endogenous) respiration was measured in 1 million cells placed in DMEM. The inhibition of the respiration was performed by the addition of 2 drugs, antimycin (5 μM) and rotenone (0.1mM).

Real-Time Quantitative PCR

Extraction of DNA from primary culture cells was performed using a blood and tissue kit (Qiagen), following the manufacturer's instructions.

The measurement of mitochondrial DNA content by real-time quantitative PCR was performed using IQTM SYBR Green Supermix (Bio-Rad Laboratories, Hercules, CA) on a thermocycler CFX96 Touch Real-Time PCR system (Bio-Rad), as described previously.[20]

In Silico Interpretation of Genetic Variants

Synonymous, missense, and splice site variations were systematically evaluated for modifications of exonic splicing enhancer (ESE; ESE Finder 3.0 algorithm available at rulai.cshl.edu/cgi-bin/tools/ESE3/esefinder.cgi) or splicing consensus sequences (Splice Site Prediction by Neural Network at www.fruitfly.org/seq_tools/splice.html and Splice Score Calculation at rulai.cshl.edu/new_alt_exon_db2/HTML/score.html). Multiple alignments of *SACS* orthologs in various species (*Homo sapiens, Macaca mulatta, Canis lupus familiaris, Ailuropoda melanoleuca, Equus caballus, Mus musculus, Rattus norvegicus, Bos taurus, Ornithorhynchus anatinus, Gallus gallus, Anolis carolinensis, Danio rerio)* were performed using ClustalW software (www.ebi.ac.uk/Tools/msa/clustalw2/) for the analysis of the conservation of affected amino acids. The possible impact of missense variations was predicted with PolyPhen-2 (genetics.bwh.harvard.edu/pph2/), Mutation Taster (www.mutationtaster.org/), SIFT (sift.jcvi.org/www/SIFT_enst_submit.html), and PROVEAN software (provean.jcvi.org/genome_submit.php).

Detection of Gene Dosage Anomalies

We used a custom targeted 44K Agilent array to fine map the breakpoints of the deletions. Custom arrays comprised 40,582 probes, with 2,939 probes covering 800kb of the 13q12 region including the *SACS* gene (median resolution of 270 base pairs between 2 probes). Array CGH analyses were performed as described previously.[21]

Microsatellite Markers Analysis

Haplotypes of 3 patients carrying the same p.R272H missense homozygous variant were defined using 4 microsatellite markers flanking *SACS* on chromosome 13 (D13S232, D13S292, D13S787, and D13S1243), and 1 intragenic marker. The intragenic marker was searched for in the complete *SACS* genomic sequence using Repeat Masker software (www.repeatmasker.org/). We found a GT repeat in the first intron. Specific primers were then designed with primer3 (forward 5′-CACACCCTTTTTGCTGAAGG-3′ and reverse 5′-CGCATGGCAATATCACAGTC-3′ at biotools.umassmed.edu/bioapps/primer3_www.cgi). Following amplification by PCR, fluorescently labeled products were analyzed on an ABI Prism 3130XL automated sequencer. Peak analysis was performed by Genemapper Analysis Software (ABI).

Results

Identification of Point Mutations

Direct sequencing of *SACS* performed in 321 index patients from the SPATAX network allowed us to identify 60 variants not referred to as polymorphisms in the databases (dbSNP, 1000 Genomes) in 50 patients (15.6%, n = 50 of 321) and in 7 of their relatives also included in this study (Table 1, Supplementary Tables 1–3). According to earlier recommendations on variant classification graded in a 5-class system,[22] 29 nonsense or indel variants expected to lead to a premature termination codon were classified as VUS class 5 (definitely pathogenic), all of them novel except p.R2119*, p.Y3430*, and p.R3792*.[23–25] One variant was a new splicing mutation in intron 5 (c.457 + 3A>C) that dramatically decreased the score of the donor splice

TABLE 1. Molecular Genotype and Main Clinical Data for the 39 Index Cases

SPATAX Patients	Protein change		Age at onset, yr	Disease Duration, yr	Triad			Additional Signs	VUS class[a]	
					PS	A	PNP			
Nonsense homozygous variants										
AAD-366-003	p.E36*		Infancy	29–32	+	+	+	Deafness	Class 5	
AAR-270-006	p.G209Vfs*6		3	33	+	+	+	ID; altered AEP	Class 5	
AAR-330-018	p.L950Lfs*20		8	22	+	+	+	Hearing loss	Class 5	
AFT-079-003	p.R961*		1	27	+	+	+	ID; retinopathy	Class 5	
AAR-321-004	p.E1974*		0	18	+	+	ND	Mild ID	Class 5	
AAR-104-008	p.Y2210*		1.5	32.5	+	+	ND	ND	Class 5	
MAR-7444-007[b]	p.Y3430*		1	30	+	+	ND	Mild ID	Class 5	
AAR-509-001	p.K3867Nfs*1		1.5	14.5	+	+	+	ID	Class 5	
Missense homozygous variants										
AAR-456-005	p.R272H		1	20	+	+	+	–	Class 4	
FSP-269-006	p.R272H		0	33	+	+	+	ID; hearing loss	Class 4	
AAR-437-014[b]	p.R272H		1	25	+	+	ND	Mild ID	Class 4	
AAR-242-003[b]	p.I513V		22	30	+	+	+	Dystonia	Class 2	
AAR-1168-013	p.M1311K		4	39	+	+	+	Hearing loss	Class 4	
FSP-770-010	p.Y1921D		1	36	+	+	ND	ID	Class 4	
AAR-519-001[b]	p.P2099L		8	31	+	+	+	ND	Class 4	
AAR-599-001	p.R2703H		3	13	+	+	+	ID	Class 4	
AAR-235-003	p.G3843V		1	51	+	+	+	ND	Class 4	
Nonsense compound heterozygous variants										
AAR-601-003[b]	p.L143Lfs*10	p.Q4356*	1	28	+	+	+	Epilepsy; hearing loss	Class 5	Class 5
AAR-230-005	NA	p.R2119*	7	23	+	+	+	ID	Class 5	Class 5
AAR-246-003	p.I1110Nfs*1	p.E4309*	1.5	14.5	+	+	ND	ND	Class 5	Class 5
BOR-090711-003[b]	p.L1180Lfs*7	p.K3747*	25	23	+	+	+	–	Class 5	Class 5
AAR-225-008	p.R1645*	p.Y1671Lfs*20	6	33	+	+	ND	–	Class 5	Class 5
AUS-553090795-003	p.L1922Rfs*2	p.T2316Nfs*6	1	15	+	+	+	Mild ID; epilepsy	Class 5	Class 5
AAR-545-003[b]	p.V3545Efs*3	p.R3792*	3	18	+	+	+	Dystonia	Class 5	Class 5

Thierry DEFFOIN FSP-1168-013 il est FSP et pas AAR faute de frappe ici!

Celine BONAN né GOLLIN 6/8/82, erreur, patient 019 et pas 003

TABLE 1: Continued

SPATAX Patients	Protein change		Age at onset, yr	Disease Duration, yr	Triad			Additional Signs	VUS class[a]	
					PS	A	PNP			
Nonsense and missense compound heterozygous variants										
AAR-410-001	p.R276C	p.S4440*	5	37	+	+	+	ND	Class 4	Class 5
SAL-399-003	p.S365Afs*6	p.Q2605H	30	12	+	+	+	ID; altered AEP	Class 5	Class 4
AAR-334-009[b]	p.R961*	p.R2703H	0	32	+	+	+	Mild ID	Class 5	Class 4
AAD-399-077	p.M1573R	p.H2743Tfs*10	Infancy		+	+	+	−	Class 2	Class 5
AAR-491-001	p.P1583R	p.V2033Vfs*5	18	6	+	+	+	Mild ID	Class 4	Class 5
AFT-068-005[b]	p.F2056Ffs*21	p.P2217Q	1	52	+	+	+	−	Class 5	Class 4
AAR-429-003	p.S2101fs*13	p.L4451P	1	15	+	+	+	ND	Class 5	Class 4
FSP-084-009	p.Y2210*	p.P2849L	1	28	+	+	+	Mild ID	Class 5	Class 4
FSP-1171-001	p.R2425P	p.I3755Mfs*7	12	24	+	+	+	ND	Class 4	Class 5
Nonsense heterozygous variant										
ANG-120054380-003[b]	p.C1285Lfs*8		1	15	+	+	ND	Retinopathy	Class 5	

ATAXIC Patients	Protein change		Age at onset, yr	Disease Duration, yr	Triad			Additional Signs	VUS class[a]	
					PS	A	PNP			
Nonsense homozygous variants										
01017AI-003	p.V590Afs*55		1	8	+	+	+	Altered AEP	Class 5	
13003TL-003	p.Y1564*		1	11	+	+	+	ND	Class 5	
Nonsense compound heterozygous variants										
10012RB-003	p.V590Afs*55	p.K1717Nfs*8	1	13	+	+	+	Epilepsy, hypotonia	Class 5	Class 5
13006CD-003	p.G435*	p.R3546Rfs*4	1	11	−	+	ND	ID	Class 5	Class 5
Nonsense and missense compound heterozygous variants										
01023MO-003	p.Q4413Hfs*38	p.A4469D	1.5	6.5	−	+	ND	Altered AEP	Class 5	Class 3

[a]Pathogenicity class according to Plon et al.[22]
[b]Patients investigated for mitochondrial network.
+ = present; − = absent; A = ataxia; AEP = auditory evoked potential; ID = intellectual disability; NA = not applicable, splice site variant; ND = no data; PNP = polyneuropathy; PS = pyramidal signs; VUS = variants of uncertain clinical significance.

site of exon 5 (0.57 vs 1 for the wild type), when analyzed with Splice Site Prediction by Neural Network. Moreover, Mutation Taster analysis predicted this variant as pathogenic; therefore, we classified it as a VUS class 5. The remaining 30 variants were 25 missense variants (including 14 classified as VUS class 4 [likely pathogenic], 3 variants as VUS class 3 [uncertain pathogenicity], and 8 as VUS class 2 [likely not pathogenic]) and 5 synonymous variants classified as VUS class 1 (not pathogenic). Four of the VUS class 4 variants were reported previously: p.R272H, p.R276C, p.M1311K, and p.P1583R.[12,26–28] In our series, p.R272 was substituted in 3 unrelated index patients with different geographical origins (AAR-456-005, AAR-437-014, and FSP-269-006). Analyses of microsatellite markers located in or close to *SACS* revealed 3 different haplotypes (Table 2), arguing against a founder effect related to an ancestral mutation. In 17 patients, variants were in the homozygous state, whereas 16 patients were compound heterozygous (see Supplementary Table 1). In addition, we noted a single heterozygous variant in 17 patients, missense variants in 11 patients, and synonymous variants in 5 patients (see Supplementary Table 2). Patient ANG-120054380-003 carried a single heterozygous frameshift of VUS class 5, with normal customized array CGH (Fig 1) and mRNA analyses (data not shown). This truncating mutation was maternally inherited and also present in his affected sister. The segregation of mutations was demonstrated in all 7 available SPATAX families, in whom index cases carried 2 VUS class 4 and 5, adding 6 affected relatives to our large series of patients (see Supplementary Table 3).

Next generation sequencing in 156 patients with congenital ataxia from the ATAXIC project led us to identify 7 mutations in 5 index patients (3.2%, n = 5 of 156) and in 1 relative (see Table 1, Supplementary Table 1). All mutations were confirmed by Sanger direct sequencing and included 6 truncating mutations, either nonsense or ins/del, and 1 missense VUS class 3. The substituted residue was highly conserved during evolution, and in silico prediction showed modification of ESE scores. Mutations were demonstrated to segregate in the 2 available ATAXIC families (see Supplementary Table 3).

Sanger direct sequencing of DNA and cDNA of Patient 12436B-JAM-001, carrying the genomic deletion (see Fig 1), failed to find a second point mutation.

Characterization of the Mitochondrial Network Morphology

Primary culture of skin fibroblasts was performed from 8 controls, 5 females and 3 males of various ages. We first compared the mitochondrial network morphology between all the controls. The observed proportions of cells with abnormal fused mitochondria were very similar in all the experiments, demonstrating that mitochondrial morphology could be reliably analyzed and did not vary according to sex and age (Fig 2B). Thus, we used 1 male and 1 female control to compare their mitochondrial networks with 11 patients carrying different types of variations: 8 patients carrying biallelic VUS exclusively of class 5 and 4 (MAR-7444-007, BOR-090711-003, AAR-545-003, AAR-601-003, AAR-437-014, AAR-519-001, AAR-334-009, and AFT-068-005), 1 patient (AAR-242-003) with a homozygous VUS class 2 (mutation p.I513V), Patient ANG-120054380-003 with a cosegregating monoallelic VUS class 5, and Patient 12436B-JAM-001 with a genomic deletion. Skin fibroblasts of all patients but 1 (12436B-JAM-001) displayed altered mitochondrial morphology, with a significant increase of bulbed mitochondria as compared to controls (see Fig 2). We also performed a relative quantification of the global mass of the mitochondrial network using fluorescence intensity measurement of the MitoTracker labeling, except on Patient AAR-437-014 (Fig 3A). All patients, except 12436B-JAM-001, displayed a decrease of the mitochondrial mass ranging from 17% to 55% (see Fig 3B). To confirm this decrease, we quantified the mitochondrial and nuclear DNAs using quantitative PCR assays. The mtDNA/nDNA ratio analysis revealed a decrease of mtDNA quantity ranging from 14% to 67%, concordant with the results of fluorescence experiments (see Fig 3C).

We observed a defect in MitoTracker incorporation in fibroblasts of Patient AAR-437-014 (see Fig 3E). The abnormal fluorescence in these fibroblasts was possibly related to $\Delta\Psi$m anomalies. To measure $\Delta\Psi$m, the potential-sensitive dye TMRM is classically used. Fibroblasts of Patient AAR-437-014 revealed a decrease of 30% ± 4% in TMRM fluorescence (see Fig 3F). This result suggests an impaired mitochondrial energetic function in this patient.

To verify any mitochondrial energetic deficiency, we analyzed mitochondrial oxygen consumption in 5 patients (AAR-242-003, AAR-437-014, AAR-545-003, AFT-068-005, and ANG-120054380-003) carrying different classes of VUS. No modification of basal oxygen consumption rate was observed in 4 of them, but the mitochondrial oxygen consumption was strongly reduced (51% ± 5%) in the fibroblasts of AAR-437-014 (see Fig 3D), in agreement with the observed alteration of $\Delta\Psi$m.

Clinical and Paraclinical Characteristics of ARSACS Patients

The diagnosis of ARSACS was finally established in 34 index patients from SPATAX (10.6%, n = 34 of 321) and in 5 index patients from the ATAXIC cohort (3.2%,

TABLE 2. Haplotype Analysis around *SACS*

Haplotype	Patient		
	AAR-456-005	AAR-437-014	FSP-269-006
D13S232	118-118	106-106	118-118
SACS	233-233	235-235	232-232
D13S292	130-130	134-134	130-130
D13S787	256-256	253-253	256-256
D13S1243	253-253	255-255	250-253

Haplotype analysis using 4 flanking and 1 intragenic microsatellite markers on 3 patients carrying the same mutation, p.R272H. Numbers for haplotypes represent the size of polymerase chain reaction products in bp.

n = 5 of 156). In addition, 8 affected relatives (including the sister of Patient ANG-120054380-003) were also included in our clinical study. Overall, a total of 47 ARSACS patients from 39 families were included (Supplementary Table 4). Twenty-two probands were from France, including 2 patients with origins associated with either Maghreb or Poland; 8 were from Algeria; 2 from Morocco; 2 from Portugal; 1 each from Australia, Italy, and Turkey; and 2 of unknown origin. Consanguinity was reported in 26% (n = 10 of 39); 62% of affected individuals (n = 29 of 47) were females, and 38% (n = 18 of 47) were males.

The mean age at onset was 5.1 ± 7.4 years, ranging from birth to age 30 years; 83% had onset before the age of 10 years and 72% before 5 years of age (Supplementary Tables 4 and 5). Notably, 5 index patients and 1 relative displayed a phenotype of congenital ataxia and 2 patients presented an atypical late onset after 25 years. Unsteadiness was the most frequent feature at onset (96%; n = 43 of 45) either isolated (82%; n = 37 of 45) or associated with stiff legs (11%; n = 5 of 45). Only 2 patients complained of isolated stiff legs at onset (5%, n = 2 of 42). The mean age of patients at examination was 29.7 ± 12.9 (range = 8–53) years, and the mean disease duration was 24.3 ± 12.5 years. According to the Spinocerebellar Degeneration Functional Score (SDFS), which rates the disability stages from 0 (asymptomatic) to 7 (bedridden),[29] 17% of our patients (n = 7 of 42) were mildly (SDFS = 1–2) affected (mean age = 21.3 ± 14.6 years), 28% (n = 12 of 42) were moderately (SDFS = 3) affected (mean age = 27.7 ± 12.0 years), and 55% (n = 23 of 42) were severely (SDFS = 4–7) affected (mean age = 35.2 ± 10.5 years), including 8 wheelchair bound and 1 bedridden (mean age = 36.5 ± 12.6 years, range = 16–53). After age 30 years, 25% of the patients (n = 6 of 24) were wheelchair bound. Frequencies of the different features are presented in Supplementary Table 5. All patients had static and kinetic ataxia. Spasticity was present in 63% in lower limbs and 12% in upper limbs. Hearing loss, abnormal auditory evoked potentials, and epilepsy were rarely noted. Difficulties at school possibly related to mild intellectual disability were noted in 51% of patients, but neuropsychological evaluations were very rarely available (see Supplementary Tables 4 and 5). Fundus examination was available for 16 patients and detected retinal nerve fiber layer hypertrophy of axonal fibers in only 3 of them (19%). In these patients, retinal nerve fiber hypertrophy was more pronounced close to the optic disk in its superior and inferior parts rather than the nasal and temporal regions (Fig 4). In 2 of them (Patients ANG-120054380-003 and AUS-553090795-003), these clinical data were confirmed by optical coherence tomography. Brain MRI was performed in 41 patients and was considered normal in 2 of them (AAR-491-001 and AAR-321-007, but performed at age 7 years in the latter case). Vermis atrophy with upper predominance was found in 39 patients, whereas cerebellum hemispheres were affected in 23. T2/fluid-attenuated inversion recovery (FLAIR) linear hypointensities were detected in the pons in 19 patients, and lateral hyperintensities and enlargement of middle cerebellar peduncles were present in 7 and 9 patients, respectively. Perithalamic T2/FLAIR hyperintensities were noted in 5 patients (see Fig 4). Electromyoneurography revealed sensorimotor polyneuropathy in 97% of patients (n = 36/37), either axonal (n = 9/36, 25%), demyelinating (n = 19/36, 53%), or both (n = 5/36, 14%); no precise data were available for the 3 remaining patients.

Among the 6 patients with a phenotype of congenital ataxia, mean age at onset was 1.1 ± 0.1 years and mean age at evaluation was 10.7 ± 2.3 years. The mean disease duration was 9.6 ± 7.4 years, leading to a mild disability score (SDFS = 2) in the 3 patients for whom the data were available. The oldest patient from this group was a 14-year-old boy (10012RB) who manifested

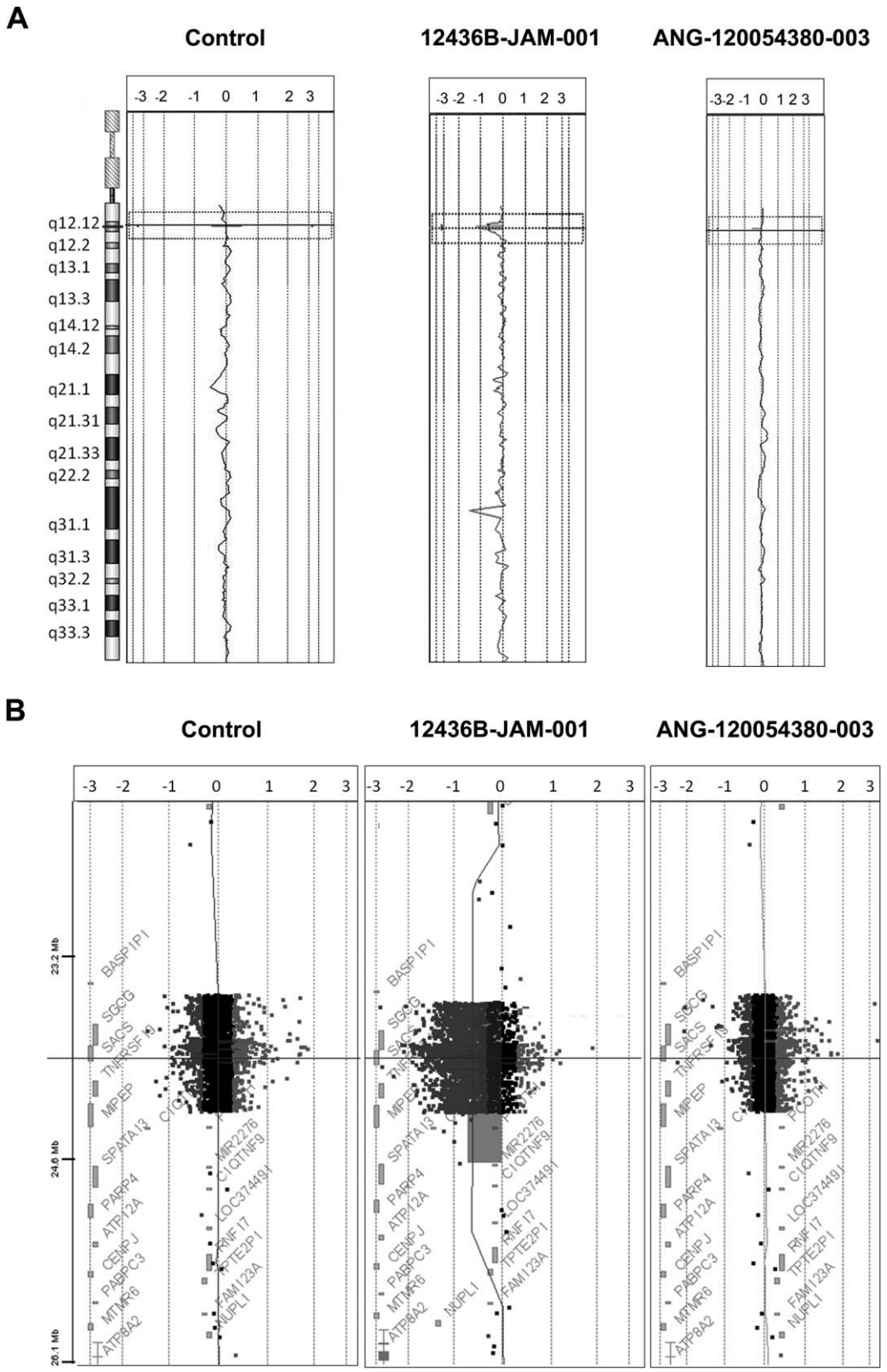

FIGURE 1: Array comparative genomic hybridization analysis on Patient ANG-120054380-003 (carrying 1 truncating mutation) and Patient 12436B-JAM-001. (A) Chromosomal view showing a deviation of the baseline for Patient 12436B-JAM-001 consistent with a deletion in the 13q12 region, which is absent in the control and Patient ANG-120054380-003. (B) Close-up of the 13q12.12 region. For Patient 12436B-JAM-001, the light gray points indicate the deleted region comprising the *SACS* gene, where the average log2 ratio is about −1. For the control and Patient ANG-120054380-003, the lines show the absence of alteration in this region.

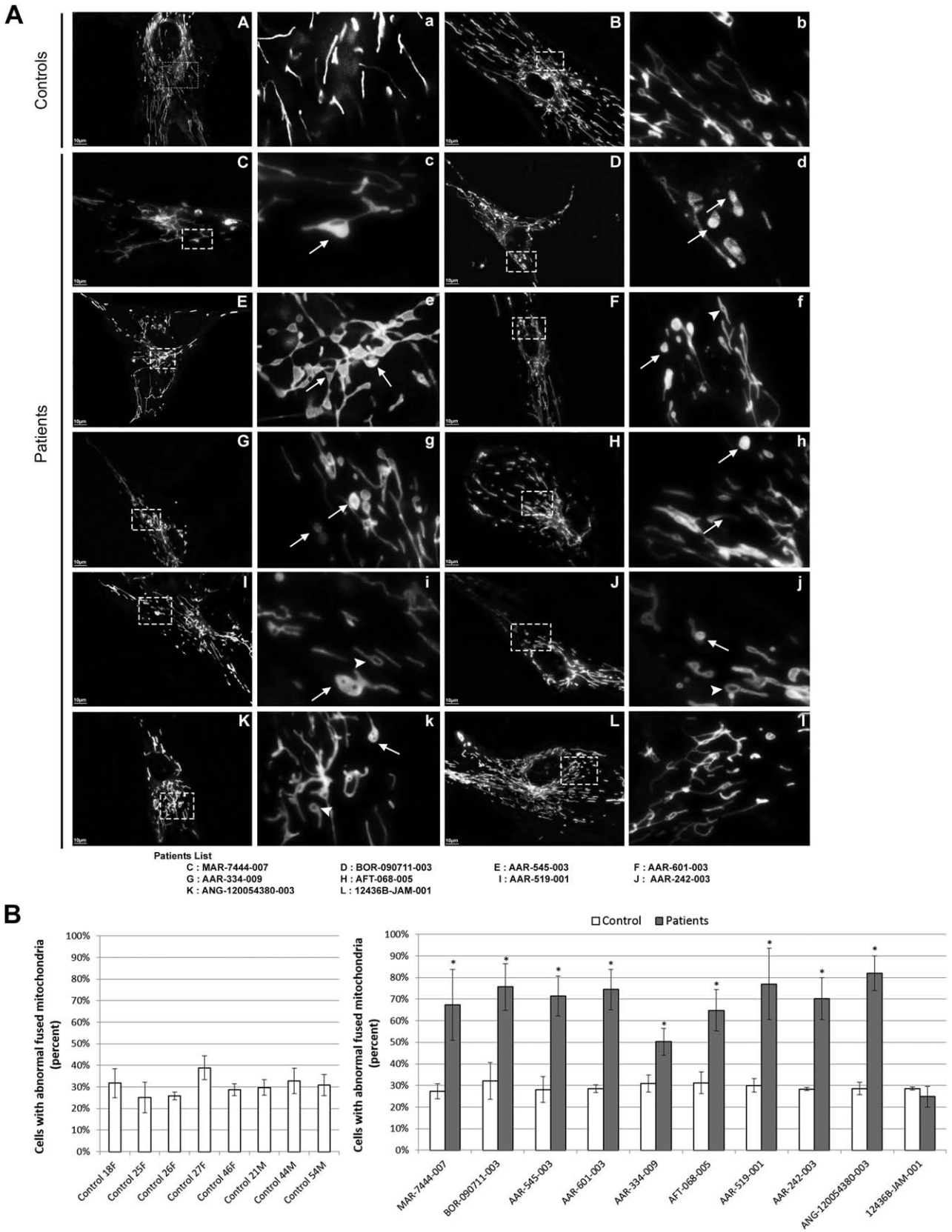

FIGURE 2: Mitochondrial network using MitoTracker labeling. (Upper panel A) The mitochondrial network of the autosomal recessive spastic ataxia of Charlevoix–Saguenay (ARSACS) patients' skin cells was observed by fluorescence microscopy (C–K) and revealed hyperfused tubules as compared to control skin fibroblasts (A, B). Magnified images are presented (a–k) and show the balloon-like *(arrows)* and the bulbed mitochondria *(arrowheads)* characteristic of a hyperfused phenotype. (Lower panel B) Around 100 cells from 3 independent experiments were analyzed. (Left) Balloon-like and bulbed mitochondria were counted for 8 different controls, 5 females (F) and 3 males (M) of various ages. Because similar results were obtained for all the controls, only 2 of them (46F and 21M), were used to compare with patients. (Right) Balloon-like and bulbed mitochondria were counted for 2 controls and 10 patients. The 95% confidence interval around the mean was computed for each control and the percentage of patients' cells presenting more abnormal fused mitochondria than the upper limit of the 95% confidence interval is presented as mean ± standard error of the mean. A Mann–Whitney test was used for statistical analysis $*p \leq 0.05$.

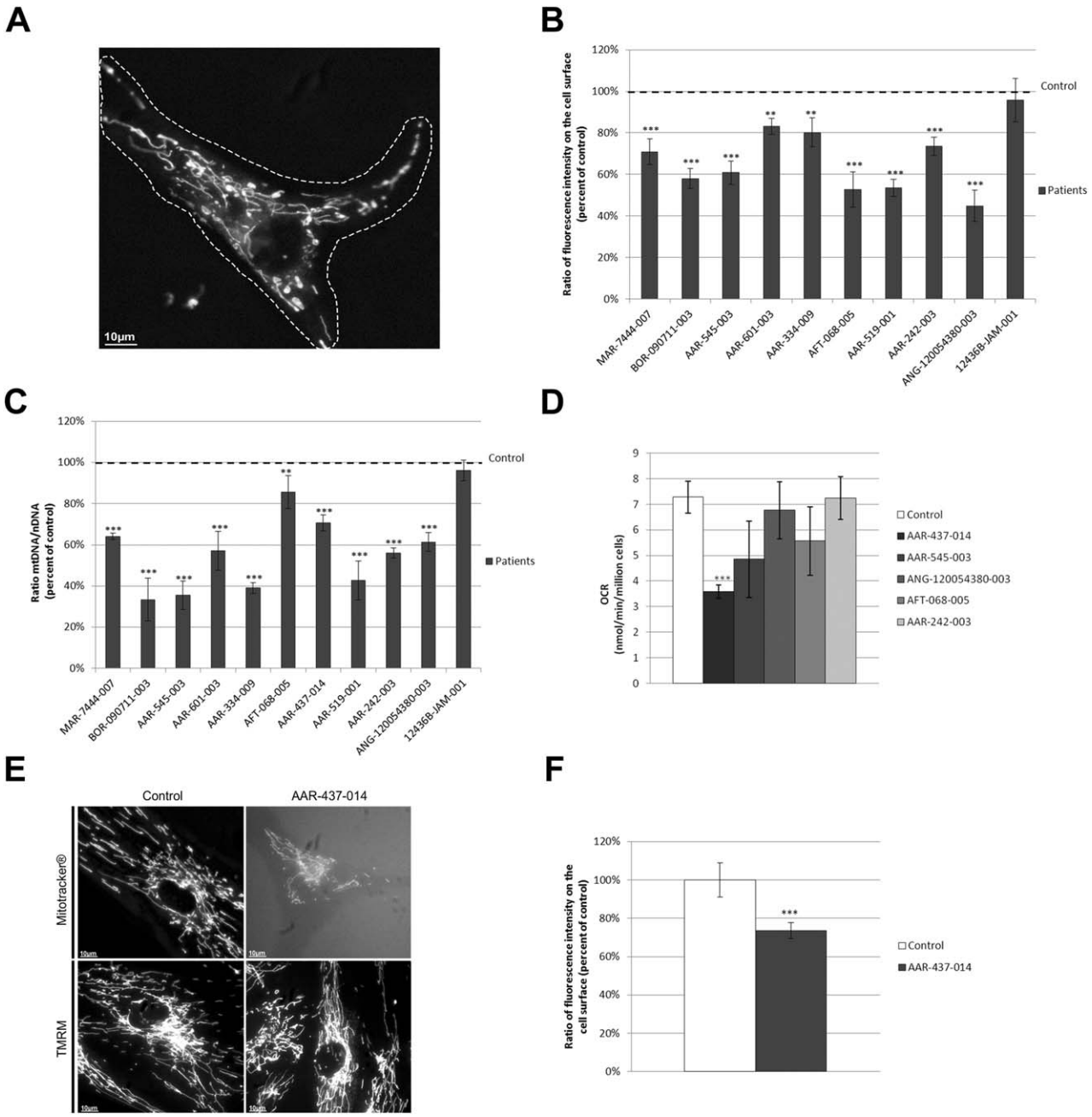

FIGURE 3: Mitochondrial abnormalities in skin fibrobasts. Cells obtained from the patients (A) and the control were labeled using MitoTracker Green to measure the whole cell surface. (B) Fluorescence intensity was measured for 10 ARSACS patients and 1 control. The quantification was performed with ImageJ (n = 3; >100 cells). (C) The mtDNA was quantified by quantitative polymerase chain reaction in 11 ARSACS patients and the control (n = 3). (D) The mitochondrial respiration (oxygen consumption rate [OCR]) was quantified by oxygraphy in 5 patients (n = 3). (E) Following the abnormal fluorescence observed with the MitoTracker labeling, fibroblasts of the control and Patient AAR-437-014 were incubated with tetramethylrhodamine methyl ester (TMRM), and (F) the fluorescence intensities were quantified by ImageJ software (n = 3; >100 cells). Data are presented as mean ± standard error of the mean; **$p < 0.01$, ***$p < 0.001$. Significance was determined using a 1-tailed unpaired *t* test.

only a very early nonprogressive mild static and kinetic ataxia (Scale for the Assessment and Rating of Ataxia evaluated at 6/40 at age 14 years) associated with partial epilepsy that occurred at age 10 years, demyelinating sensorimotor neuropathy, and linear hypointensities in the pons and upper vermis atrophy on brain MRI.

Discussion

ARSACS is currently considered to be among the most frequent types of spastic ataxia worldwide after Friedreich ataxia and ataxia telangiectasia.[4,5,9,29] Most of the *SACS* mutations described outside Quebec are private, with an increasing number of missense variants described since

2008.[4,5,9] Because a deleterious effect of these missense variants has rarely been demonstrated through functional assays,[14,30] they would have been classified as VUS rather than pathogenic mutations.[5,22] Because false assignments of pathogenicity can bring about serious consequences for patients, in terms of prognostic, therapeutic, and/or reproductive advice, most of the guidelines for implicating sequence variants in human disease more often advise experimental approaches to investigate the impact of a sequence variant on gene function or cell or organism phenotype. Moreover, the guidelines strongly suggest that evidence derived directly from patient tissue or cells, rather than model systems, could be particularly informative.[31] The main goal of our work was to identify a trait biomarker specific to ARSACS crucial for helping to validate VUS $\leq$ class 4 in *SACS* as true mutations, based on a large series of ARSACS patients from 2 separate cohorts of ataxic patients.

In the first step, we identified biallelic *SACS* variants in 38 families, with 33 of 321 index cases (10.2%) presenting with sporadic or autosomal recessive ataxia and spasticity with onset at <45 years and 5 of 156 probands with congenital ataxia (3.2%), that is, patients presenting with very early onset nonprogressive ataxia or with a tendency to improve with age (see Table 1). Importantly, half of these variants were VUS $\leq$ class 4, leading to uncertain interpretation. A great majority were novel, although we also found some recurrent variants, including p.R272H identified in 3 unrelated families. Our findings, together with the previous reports of p.R272C in 4 Canadian families[32,33] and p.R272H in an Italian family,[28] reveal p.R272 as a mutational hotspot in *SACS*. Alternatively, we also identified some patients who carried a single heterozygous *SACS* variant (see Supplementary Table 2). Notably, a unique patient (ANG-120054380-003) was demonstrated to carry a heterozygous nonsense mutation (VUS class 5) inherited from his mother and also carried by his affected sister (see Supplementary Table 1). Finally, Patient 12436B-JAM-001, carrying a heterozygous genomic deletion encompassing the whole *SACS* gene, had no additional point mutation on the second allele. These results may suggest that the second mutation remained undetected because it is located in parts of the gene that have not been analyzed, that is, regulatory regions upstream of the gene or deep in the introns. However, because array CGH analysis could not be performed on these patients, we cannot rule out a possible deletion in the second allele, even if we checked the heterozygous state of the numerous SNPs present in *SACS*. Finally, we cannot exclude the possibility that these patients may be affected by other ataxias.

According to the suggested role of sacsin in the maintenance of mitochondrial morphology and function,[13,15,16] we analyzed whether morphological and functional alterations of mitochondria occurred in primary cultures of skin fibroblasts. We found a drastically altered mitochondrial network with numerous balloon-like or bulbed mitochondria in 10 of the 11 studied patients, including 8 patients harboring 2 VUS of class 4 or higher, Patient AAR-242-003 carrying a homozygous VUS class 2, and Patient ANG-120054380-003 harboring a single heterozygous VUS class 5 (see Table 1, Fig 2). Conversely, in Patient 12436B-JAM-001, carrying a heterozygous genomic deletion comprising the *SACS* gene, we did not find any mitochondrial abnormalities. These results confirm previous observations in other cell types including immortalized skin fibroblasts from 2 ARSACS patients,[13,15] and more recently in fibroblasts from a patient carrying missense compound heterozygous variants,[34] and strongly suggest that an abnormally fused mitochondrial network is a distinctive phenotype in primary culture of fibroblasts of ARSACS patients.

Together with the alteration of mitochondrial morphology, we also measured a concomitant decrease of mitochondrial mass. However, these alterations had no impact on the global mitochondrial respiratory function. Girard et al[15] reported that sacsin is required for normal mitochondrial function but not for mitochondrial respiratory function. However, we observed that fibroblasts carrying the p.R272H homozygous missense mutation (AAR-437-14) displayed altered mitochondrial respiration, membrane potential, and morphology. This mutation is located in the sub-repeat 1 (sr1) domain of sacsin. Sacsin contains 3 sr domains (sr1–3),[14] which form the SIRPTs (Sacsin Internal RePeaTs).[12] This sr1 contains a histidine kinase-like adenosine triphosphatase, and mutations in this domain display a higher SPAX score, which evaluates phenotype severity.[12] These data support our findings that p.R272 might play an important role in the sacsin-dependent mitochondrial phenotype. It would be interesting to analyze whether the 2 other families carrying this mutation display the same severe mitochondrial phenotype.

Strong evidence has emerged to indicate disturbed mitochondrial fusion and fission as central pathological processes involved in several childhood and adult onset neurodegenerative disorders.[35] Such abnormalities have been reported in the dominant form of spinocerebellar ataxia SCA28 (OMIM #614206), in which inactivation of *AFG3L2* in mouse cortical neurons resulted in mitochondrial fragmentation.[36] Opposite observations of an elongated mitochondrial network have been demonstrated in patients' fibroblasts with hereditary spastic

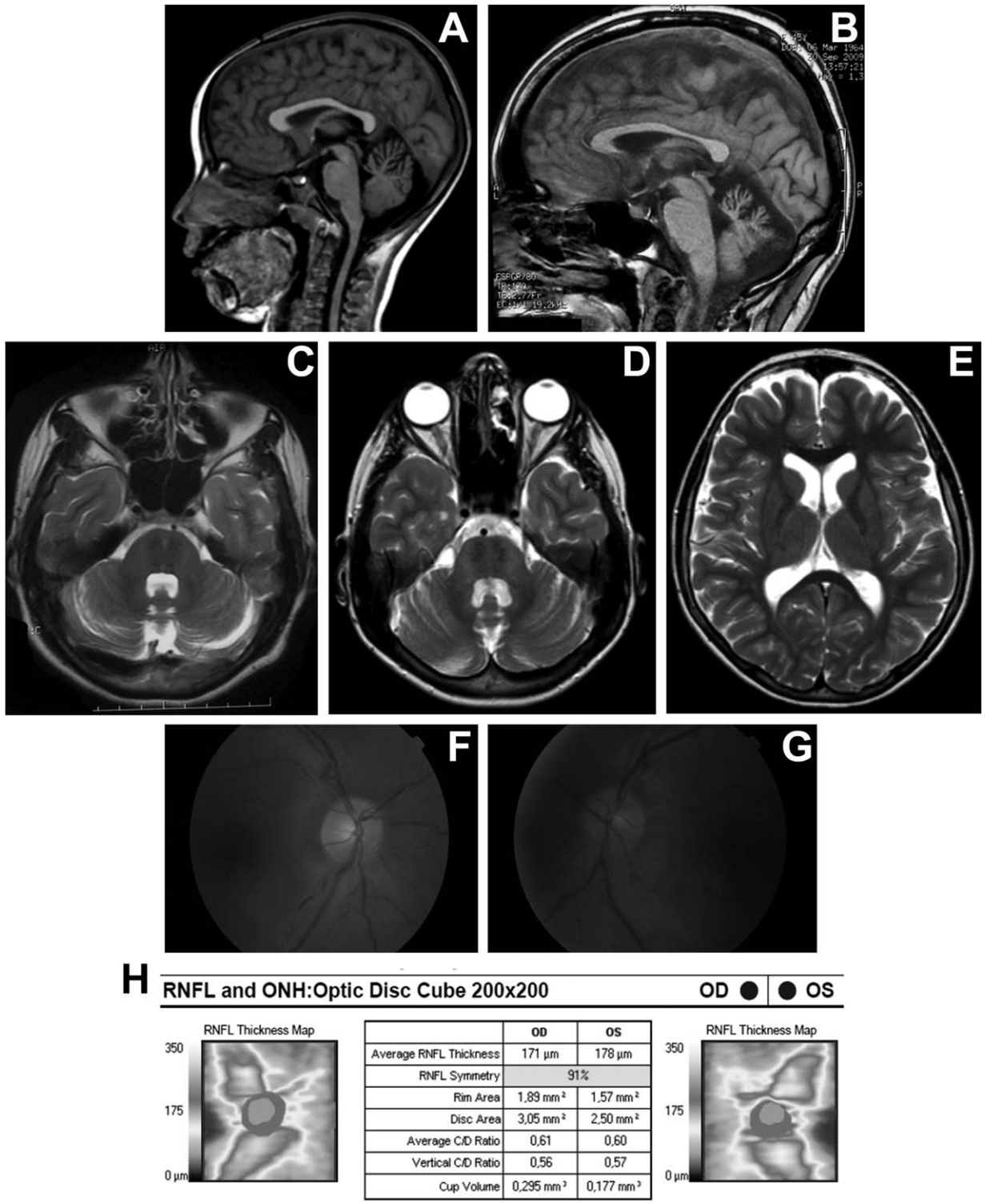

	OD	OS
Average RNFL Thickness	171 µm	178 µm
RNFL Symmetry	91%	
Rim Area	1,89 mm²	1,57 mm²
Disc Area	3,05 mm²	2,50 mm²
Average C/D Ratio	0,61	0,60
Vertical C/D Ratio	0,56	0,57
Cup Volume	0,295 mm³	0,177 mm³

FIGURE 4: Brain magnetic resonance imaging of several ARSACS patients exhibiting characteristic features and ophthalmological findings in Patient ANG-120054380-003. T1 sagittal cross-sections demonstrate predominant upper vermis atrophy in Patients 01017AI at age 6 years (A) and BOR-090711-003 at age 45 years (B). T2 axial cross-sections show linear pons hypointensities in Patients BOR-090711-003 at age 42 years (C) and 10012RB at age 14 years (D). Note the mild enlargement of the middle cerebellar peduncles (MCP) in BOR-090711-003 (C) and mild hyperintensity of the MCP in 10012RB (D). (E) T2 axial cross-section at the level of basal ganglia showing peripheral hyperintensities surrounding thalami in 10012RB at age 14 years. Retinal fundus images in the right (F) and left (G) eye disclose abnormally visible retinal axons, due to ganglion cell and retinal nerve fiber hyperplasia, detectable close to the optic disk. (H) Optical coherence tomography of the optic nerve heads (ONH), displaying thickening of the retinal nerve fiber layers (RNFL), in the right eye (OD) and the left eye (OS), in Patient ANG-120054380-003. C/D = cup-to-disk.

TABLE 3. New Definitions for Establishing a Diagnosis of ARSACS

Definition	Diagnostic Criteria
Possible ARSACS	Spastic ataxia or congenital ataxia or spastic paraplegia **AND** 2 VUS $\leq$ class 4 in *SACS*
Probable ARSACS	Spastic ataxia or congenital ataxia or spastic paraplegia **AND** 1 VUS class 5 with 1 VUS $\leq$ class 4 in *SACS*
Definite ARSACS	Spastic ataxia or congenital ataxia or spastic paraplegia **AND** 2 VUS class 5 in *SACS* **OR** at least 1 VUS class 5 or 2 VUS $\leq$ class 4 in *SACS* and altered mitochondrial network in fibroblasts

VUS = variants of uncertain clinical significance.

paraplegia type 7 (SPG7; OMIM #607259),[37] (SPG31; OMIM #610250),[38] and SPG56 (OMIM# 615030, named SPG49 by the HUGO nomenclature).[39] The potential direct or indirect roles in the dysregulation of fission or fusion of the mutated proteins paraplegin, REEP1, and CYP2U1, respectively, are still unknown. The clinical spectrum of these latter conditions, generally dominated by a pyramidal syndrome of the lower legs with progressive spasticity, is somewhat distinguishable from ARSACS clinical presentation. A clinical picture of spastic ataxia may be observed in SPG7 with either progressive external ophthalmoplegia or ptosis and a mid-adult onset, although mild cerebellar ataxia has only been reported in a few patients with SPG31 after long duration of the disease.[37,38,40]

Regarding the clinical data, our study clearly confirms in a large series that most ARSACS patients manifest with the typical presentation following a very slowly progressive course with unsteadiness as a sign at onset, sometimes responsible for mild motor milestone delay, associated with spasticity during childhood and

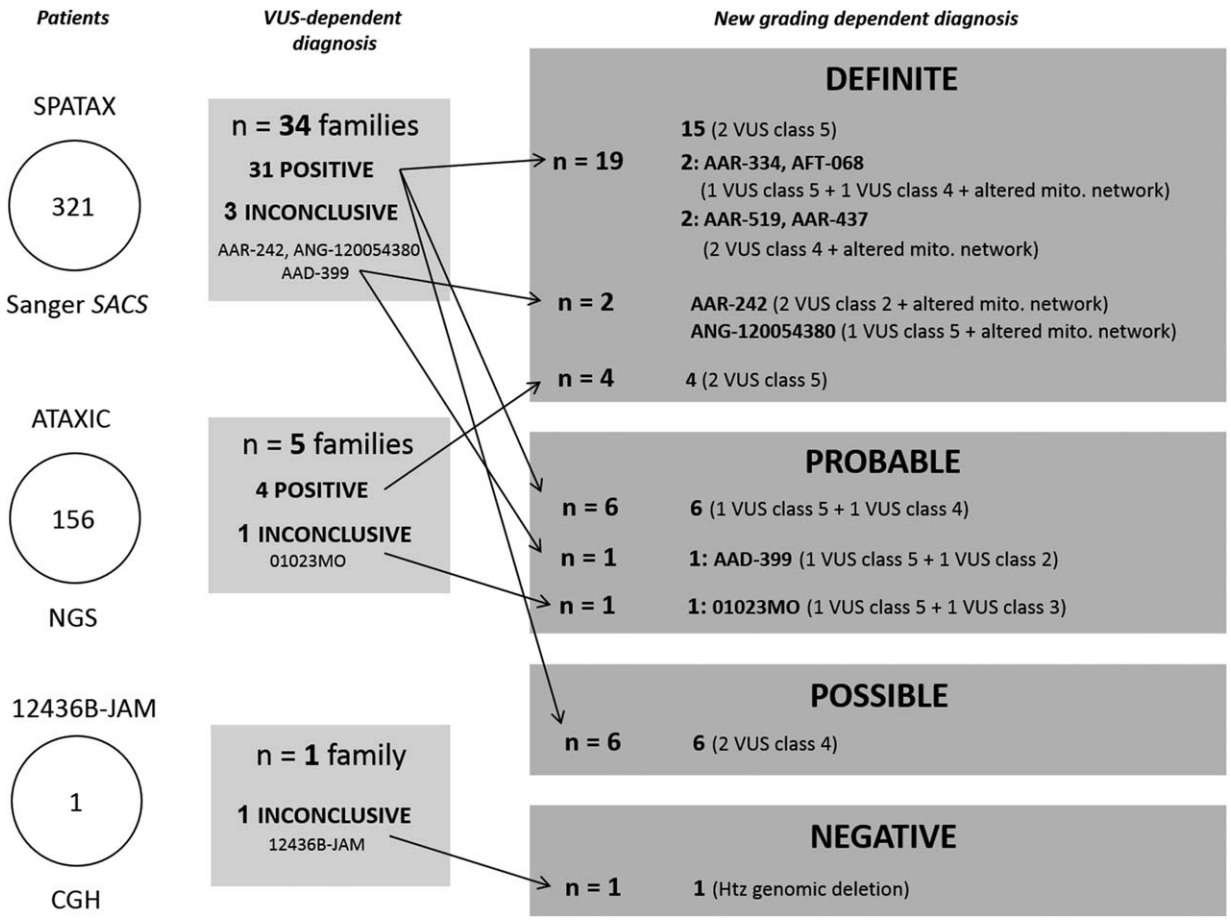

FIGURE 5: Evolution of ARSACS diagnosis in this study. Following Sanger sequencing, next generation sequencing (NGS), or array comparative genomic hybridization (CGH) analysis, 40 families were retained. Based on the VUS classification, 35 were positive and 5 were inconclusive regarding ARSACS diagnosis. According to our new definitions, including the presence of an altered mitochondrial network, 25 families were validated as definite ARSACS, 8 as probable, 6 as possible, and 1 as negative.

neuropathy during the teenage years (see Supplementary Table 5).[41] Alternatively, our findings highlight that atypical ARSACS with late onset, atypical features (such as hearing loss, increased auditory evoked potential latencies, and epilepsy), or at least 1 of the core features missing may occur (see Table 1, Supplementary Table 5).[5,9,42] Notably, the disease of 2 patients (AAR-334-009 and AAR-519-001) initiated with early onset lower limb spasticity that remained isolated for 16 and 8 years, respectively, before the occurrence of ataxia. We also extend the spectrum of atypical ARSACS to congenital ataxia (see Supplementary Table 5). The course of the disease was dramatically stable for all these patients, with the longest disease duration being 14 years. However, ARSACS patients originally described in Quebec had early onset ataxia with slow progression leading to wheelchair dependence after an average of 40 years.[10] It is possible that patients with congenital ataxia resemble this common course in Quebec. In such atypical cases, the diagnosis of ARSACS, even in the presence of 2 mutations in *SACS*, may be particularly challenging, illustrating the interest in a trait biomarker that can help lead to the diagnosis.

In summary, the classical triad associating early onset ataxia, lower limb spasticity, and peripheral polyneuropathy is frequently but not systematically found in all ARSACS patients.[5] We have expanded the spectrum of ARSACS-related phenotypes (which now encompass congenital ataxia) and mutations in *SACS*, highlighting the potential difficulties of interpreting molecular results facing atypical presentations in a routine diagnosis practice. However, VUS class ≤ 4 are frequently identified in *SACS*, leading to inconclusive molecular diagnosis in routine practice. Moreover, brain MRI and electroneuromyography anomalies—highly, but not exclusively, suggestive features of ARSACS—may be missing in some patients, and for this reason cannot be systematically used as a trait biomarker. We therefore recommend analyzing *SACS* in patients experiencing ataxia, spastic ataxia, and spastic paraplegia, independent of the age at onset, the course of the disease, and the results of paraclinical examinations. We propose new practical definitions integrating, in addition to identification of variants in *SACS*, the presence of an altered mitochondrial network in primary culture of fibroblasts as a major criterion helping to definitely establish the diagnosis of ARSACS (Table 3). Based on these new definitions, we retained the diagnosis of definite ARSACS in 31 patients (from 25 families), probable ARSACS in 8 patients (from 8 families), and possible ARSACS in 8 patients (from 6 families; Fig 5). Specifically, the presence of an altered mitochondrial network prompted us to validate the diagnosis of definite ARSACS in 2 families (AAR-242 carrying a homozygous VUS class 2 and ANG-120054380 carrying only 1 VUS class 5) and to exclude it in Patient 12436B-JAM-001, for whom molecular results would have been quite difficult to interpret in a routine diagnosis practice. It is likely that those families would have been diagnosed as not having ARSACS at all. Because next generation sequencing will become the most common molecular diagnostic tool, leading to the identification of an increasing number of VUS class ≤ 4 variants, it will be very appealing to link our proposed system to it.

Acknowledgment

This work was financially supported by the National Agency for Research (projects ANR-09-MNPS-032/SPAX and ANR 13-ISV1-0002-01/SPATAX-QUEST), French Ministry of Health (PHRC 2009, AOM 09178), Verum Foundation, Roger de Spoelberch Foundation, Rare Diseases Foundation, Strumpell-Lorrain Association (ASL) (2011-0135), Know the Cerebellar Syndromes Association (CSC), Association against Mitochondrial Diseases (AMMi), and National Union of the Blind and Visually Impaired (UNADEV).

We thank the family members who generously contributed their time and materials for this research; F. Lesne for his technical contribution; and Drs. A. Richer, F. Sedel, A. M. Tataru, A. Troiano, and S. Mohammad for their collaboration.

Authorship

J.P., I.C., and C.G. conceived the study, designed the experiments, analyzed and interpreted data, and wrote the manuscript. J.L., E. Mau. C.H., N.B., C.R., J.B., and C.M.D. performed experiments. S.M. analyzed the clinical data. R.R. and G.B. assisted with data analysis and/or experimental design. M.A., S.F., D.R., A.D., L.B., D.M., M.B., D.B., A.B., G.S., K.N., C.T.-R., C.V., G.L., M.K., N.H., J.V.-G., A.G., P.Ch., E. Mai. L.G.-M., D.H., G.F., A.A., S.C.-B., S.V., P.Co., P.B., and D.L. provided human specimens and clinical data. All authors were participants in the discussion of the results and review of the manuscript. I.C. and C.G. contributed equally to this work.

Potential Conflicts of Interest

The authors have no conflicts of interest with respect to the current work.

References

1. Bouchard JP. Recessive spastic ataxia of Charlevoix-Saguenay. In: de Jong JMBV, ed. Hereditary neuropathies and spinocerebellar atrophies. Handbook of clinical neurology, vol. 16. Amsterdam, the Netherlands: Elsevier, 1991:451–459.

2. Yamamoto Y, Hiraoka K, Araki M, et al. Novel compound heterozygous mutations in sacsin-related ataxia. J Neurol Sci 2005;239:101–104.
3. Takiyama Y. Autosomal recessive spastic ataxia of Charlevoix-Saguenay. Neuropathology 2006;26:368–375.
4. Vermeer S, Meijer RP, Pijl BJ, et al. ARSACS in the Dutch population: a frequent cause of early-onset cerebellar ataxia. Neurogenetics 2008;9:207–214.
5. Synofzik M, Soehn A, Gburek-Augustat J, et al. Autosomal recessive spastic ataxia of Charlevoix-Saguenay (ARSACS): expanding the genetic, clinical and imaging spectrum. Orphanet J Rare Dis 2013;8:41.
6. Martin M-H, Bouchard J-P, Sylvain M, et al. Autosomal recessive spastic ataxia of Charlevoix-Saguenay: a report of MR imaging in 5 patients. Am J Neuroradiol 2007;28:1606–1608.
7. Garcia-Martin E, Pablo LE, Gazulla J, et al. Retinal segmentation as noninvasive technique to demonstrate hyperplasia in ataxia of Charlevoix-Saguenay. Invest Ophthalmol Vis Sci 2013;54:7137–7142.
8. Yu-Wai-Man P, Pyle A, Griffin H, et al. Abnormal retinal thickening is a common feature among patients with ARSACS-related phenotypes. Br J Ophthalmol 2014;98:711–713.
9. Bouhlal Y, Amouri R, El Euch-Fayeche G, et al. Autosomal recessive spastic ataxia of Charlevoix-Saguenay: an overview. Parkinsonism Relat Disord 2011;17:418–422.
10. Bouchard JP, Richter A, Mathieu J, et al. Autosomal recessive spastic ataxia of Charlevoix-Saguenay. Neuromuscul Disord 1998; 8:474–479.
11. Engert JC, Bérubé P, Mercier J, et al. ARSACS, a spastic ataxia common in northeastern Québec, is caused by mutations in a new gene encoding an 11.5-kb ORF. Nat Genet 2000;24:120–125.
12. Romano A, Tessa A, Barca A, et al. Comparative analysis and functional mapping of SACS mutations reveal novel insights into sacsin repeated architecture. Hum Mutat 2012;34:525–537.
13. Parfitt D, Michael GJ, Vermeulen EG, et al. The ataxia protein sacsin is a functional co-chaperone that protects against polyglutamine-expanded ataxin-1. Hum Mol Genet 2009;18:1556–1565.
14. Anderson JF, Siller E, Barral JM. The sacsin repeating region (SRR): a novel Hsp90-related supra-domain associated with neurodegeneration. J Mol Biol 2010;400:665–674.
15. Girard M, Larivière R, Parfitt DA, et al. Mitochondrial dysfunction and Purkinje cell loss in autosomal recessive spastic ataxia of Charlevoix-Saguenay (ARSACS). Proc Natl Acad Sci U S A 2012; 109:1661–1666.
16. Larivière R, Gaudet R, Gentil BJ, et al. Sacs knockout mice present pathophysiological defects underlying autosomal recessive spastic ataxia of Charlevoix-Saguenay. Hum Mol Genet 2015;24:727–739.
17. Chazotte B. Labeling mitochondria with TMRM or TMRE. Cold Spring Harb Protoc 2011;7:895–897.
18. Frank S, Gaume B, Bergmann-Leitner ES, et al. The role of dynamin-related protein 1, a mediator of mitochondrial fission, in apoptosis. Dev Cell 2001;1:515–525.
19. Estaquier J, Arnoult D. Inhibiting Drp1-mediated mitochondrial fission selectively prevents the release of cytochrome c during apoptosis. Cell Death Differ 2007;14:1086–1094.
20. Gianotti TF, Sookoian S, Dieuzeide G, et al. A decreased mitochondrial DNA content is related to insulin resistance in adolescents. Obesity 2008;16:1591–1595.
21. Morice-Picard F, Lasseaux E, Cailley D, et al. High-resolution array-CGH in patients with oculocutaneous albinism identifies new deletions of the TYR, OCA2, and SLC45A2 genes and a complex rearrangement of the OCA2 gene. Pigment Cell Melanoma Res 2014;27:59–71.
22. Plon S, Eccles M, Easton D, et al. Sequence variant classification and reporting: recommendations for improving the interpretation of cancer susceptibility genetic test results. Hum Mutat 2008;29: 1282–1291.
23. Hara K, Shimbo J, Nozaki H, et al. Sacsin-related ataxia with neither retinal hypermyelination nor spasticity. Mov Disord 2007;22: 1362–1363.
24. Bouhlal Y, Zouari M, Ben Hamida C, et al. Autosomal recessive ataxia caused by three distinct gene defects in a single consanguineous family. J Neurogenet 2008;22:139–148.
25. H'mida-Ben Brahim D, M'zahem A, Assoum M, et al. Molecular diagnosis of known recessive ataxias by homozygosity mapping with SNP arrays. J Neurol 2011;258:56–67.
26. Ouyang Y, Segers K, Bouquiaux O, et al. Novel SACS mutation in a Belgian family with sacsin-related ataxia. J Neurol Sci 2008;264:73–76.
27. Prodi E, Grisoli M, Panzeri M, et al. Supratentorial and pontine MRI abnormalities characterize recessive spastic ataxia of Charlevoix-Saguenay: a comprehensive study of an Italian series. Eur J Neurol 2012;20:138–146.
28. Dibilio V, Cavalcanti F, Nicoletti A, et al. Sacsin-related spastic ataxia caused by a novel missense mutation p.Arg272His in a patient from Sicily, southern Italy. Cerebellum 2013;12:589–592.
29. Anheim M, Tranchant C, Koenig M. The autosomal recessive cerebellar ataxias. N Engl J Med 2012;366:636–646.
30. Koslov G, Denisov AY, Girard M, et al. Structural basis of defects in the sacsin HEPN domain responsible for autosomal recessive spastic ataxia of Charlevoix-Saguenay (ARSACS). J Biol Chem 2011;286:20407–20412.
31. MacArthur DG, Manolio TA, Dimmock DP, et al. Guidelines for investigating causality of sequence variants in human disease. Nature 2014;508:469–476.
32. Guernsey D-L, Dubé MP, Jiang H, et al. Novel mutations in the sacsin gene in ataxia patients from Maritime Canada. J Neurol Sci 2010;288:79–87.
33. Thiffault I, Dicaire MJ, Tetreault M, et al. Diversity of ARSACS mutations in French-Canadians. Can J Neurol Sci 2013;40:61–66.
34. Blumkin L, Bradshaw T, Michelson M, et al. Molecular and functional studies of retinal degeneration as a clinical presentation of SACS-related disorder. Eur J Paediatr Neurol 2015;19:472–476.
35. Burté F, Carelli V, Chinnery PF, Yu-Wai-Man P. Disturbed mitochondrial dynamics and neurodegenerative disorders. Nat Rev Neurol 2015;11:11–24.
36. Kondadi AK, Wang S, Montagner S, et al. Loss of the m-AAA protease subunit AFG_3L_2 causes mitochondrial transport defects and tau hyperphosphorylation. EMBO J 2014;33:1011–1026.
37. Pfeffer G, Gorman GS, Griffin H, et al. Mutations in the SPG7 gene cause chronic progressive external ophthalmoplegia through disordered mitochondrial DNA maintenance. Brain 2014;137(pt 5): 1323–1336.
38. Goizet C, Depienne C, Benard G, et al. REEP1 mutations in SPG31: frequency, mutational spectrum, and potential association with mitochondrial morpho-functional dysfunction. Hum Mutat 2011;32:1118–1127.
39. Tesson C, Nawara M, Salih M, et al. Alteration of fatty-acid-metabolizing enzymes affects mitochondrial form and function in hereditary spastic paraplegia. Am J Hum Genet 2012;91:1051–1064.
40. Pfeffer G, Pyle A, Griffin H, et al. SPG7 mutations are a common cause of undiagnosed ataxia. Neurology 2015;84:1174–1176.
41. Duquette A, Brais B, Bouchard J-P, et al. Clinical presentation and early evolution of spastic ataxia of Charlevoix-Saguenay. Mov Disord 2013;28:2011–2014.
42. Baets J, Deconinck T, Smets K, et al. Mutations in SACS cause atypical and late-onset forms of ARSACS. Neurology 2010;75: 1181–1188.